Earth's Future

RESEARCH ARTICLE
10.1029/2025EF007516

Increased Aerosols From Siberian Wildfires Buffered Arctic Warming During 2013–2019

Jiyuan Gao[1,2], **Yang Yang**[1,2], **Hailong Wang**[3], **Pinya Wang**[1,2], **Xu Yue**[1,2], and **Hong Liao**[1,2]

[1]State Key Laboratory of Climate System Prediction and Risk Management/Jiangsu Key Laboratory of Atmospheric Environment Monitoring and Pollution Control/Jiangsu Collaborative Innovation Center of Atmospheric Environment and Equipment Technology/Joint International Research Laboratory of Climate and Environment Change, Nanjing University of Information Science and Technology, Nanjing, China, [2]School of Environmental Science and Engineering, Nanjing University of Information Science and Technology, Nanjing, China, [3]Atmospheric, Climate, and Earth Sciences Division, Pacific Northwest National Laboratory, Richland, WA, USA

Key Points:

- Anthropogenic aerosol reductions in China, Europe, and North America led to Arctic warming
- Increases in Siberian wildfire aerosols caused strong Arctic cooling
- Regional aerosol changes outside the Arctic influenced Arctic climate via northward heat transport

Supporting Information:

Supporting Information may be found in the online version of this article.

Correspondence to:

Y. Yang,
yang.yang@nuist.edu.cn

Citation:

Gao, J., Yang, Y., Wang, H., Wang, P., Yue, X., & Liao, H. (2026). Increased aerosols from Siberian wildfires buffered Arctic warming during 2013–2019. *Earth's Future*, *14*, e2025EF007516. https://doi.org/10.1029/2025EF007516

Received 5 JUN 2025
Accepted 5 JAN 2026

Author Contributions:

Conceptualization: Jiyuan Gao, Yang Yang
Data curation: Jiyuan Gao
Formal analysis: Jiyuan Gao
Funding acquisition: Yang Yang
Investigation: Jiyuan Gao
Project administration: Hong Liao
Supervision: Yang Yang
Visualization: Jiyuan Gao
Writing – original draft: Jiyuan Gao
Writing – review & editing: Yang Yang, Hailong Wang, Pinya Wang, Xu Yue, Hong Liao

Abstract During 2013–2019, global aerosols, influenced by regional clean air actions and wildfires, changed significantly. Clean air actions in China, Europe, and North America reduced anthropogenic aerosols, whereas Siberia experienced increased wildfire aerosols due to local warm and dry conditions. South Asia exhibited mixed trends with increased emissions of sulfur dioxide (SO_2) and decreased carbonaceous aerosols. Using the Community Earth System Model version 1 (CESM1), this study investigates Arctic climate responses to these regional aerosol changes. Reductions in aerosols from China and Europe-North America resulted in Arctic warming effects of +0.18°C and +0.16°C, respectively, while changes in South Asian aerosols had a relatively small influence on Arctic climate. Increased aerosols from Siberian wildfires induced an Arctic cooling effect of −0.84°C, outweighing the warming from reduced anthropogenic aerosols. These cooling/warming effects are primarily attributed to changes in northward heat transport driven by aerosol changes outside the Arctic, rather than Arctic local radiative forcing. This research highlights the relationship between regional aerosols and Arctic climate, emphasizing a negative feedback mechanism via which increased Siberian wildfire aerosols, amidst accelerated warming in the Arctic Siberia, buffer the Arctic warming. It also implies that future Arctic warming could amplify Siberian wildfires, potentially reinforcing this negative feedback.

Plain Language Summary During 2013–2019, global aerosols changed notably due to clean air actions and increased wildfire activities. Anthropogenic aerosols declined in China, Europe, and North America, while wildfire aerosols increased in Siberia under warmer and drier conditions. In South Asia, emissions of sulfur dioxide increased, while carbonaceous aerosols decreased. While reduced aerosols in China and Europe-North America contributed to Arctic warming, increased aerosols from Siberian wildfires led to a stronger Arctic cooling effect. These Arctic warming/cooling effects were mainly driven by northward heat transport due to aerosol changes in lower latitudes. The results reveal a negative feedback mechanism: Arctic warming promotes Siberian wildfires, which then emit aerosols that help cool the Arctic, partially offsetting the warming.

1. Introduction

Global temperatures have been increasing mainly due to the steady rising of greenhouse gases (GHGs) concentrations as a result of human activities since the Industrial Revolution, including the burning of fossil fuels and changes in land use (IPCC, 2013, 2021). In particular, over the past few decades, the Arctic has experienced a significantly accelerated rate of warming compared to the global average, a phenomenon referred to as Arctic amplification (England et al., 2021; Previdi et al., 2021). Studies reported that the Arctic is warming at a rate that is two to four times of the global average (IPCC, 2013, 2021; Rantanen et al., 2022), observed in paleoclimatic records (Miller et al., 2010), observations (Bekryaev et al., 2010; Serreze et al., 2009; Wang et al., 2016), and model simulations (Davy & Outten, 2020; Holland & Bitz, 2003; Zhang et al., 2018, 2020). Various factors have been proposed to explain the underlying causes of Arctic amplification (Taylor et al., 2013). Among these factors, the ice-albedo feedback, which occurs as melting ice results in increased absorption of solar radiation, further enhancing warming in the Arctic, is widely recognized (Dai et al., 2019; Jenkins & Dai, 2021; Screen & Simmonds, 2010). Other factors include temperature feedback (Pithan & Mauritsen, 2014), cloud feedback (Taylor

et al., 2013; Zhang et al., 2018), lapse-rate feedback (Stuecker et al., 2018), oceanic heat flux transport (Beer et al., 2020), atmospheric moist intrusion (Woods & Caballero, 2016), thermal inversion (Bintanja et al., 2011; Zhang et al., 2021), and internal variability (Sweeney et al., 2023).

Arctic warming is indeed a phenomenon that occurs in response to either radiative forcing within the climate system, mainly driven by changes in climate forcers such as carbon dioxide (CO_2) and aerosols (Stjern et al., 2019; Stuecker et al., 2018), or internal variability (Sweeney et al., 2023). Since the Industrial Revolution, CO_2 concentrations have consistently shown an upward trend across the globe (IPCC, 2013, 2021). However, atmospheric aerosols have experienced notable trend shifts in various regions during the past decades. In 1980s, North America and Europe experienced reduction of aerosols and their precursors related to the implementation of clean air actions (Smith et al., 2011). Consequently, near-surface aerosol concentrations and aerosol optical depth (AOD) in these regions have declined over the past few decades, which were confirmed by ground observations, satellite measurements, and model simulations (Cherian & Quaas, 2020; Chin et al., 2014; Gao et al., 2023; Tørseth et al., 2012). Conversely, developing areas such as South Asia (SA) have continued to sustain high emission levels, leading to a notable increase in aerosols and their precursors, particularly sulfur dioxide (SO_2) (Liu et al., 2023; McDuffie et al., 2020; Samset et al., 2019), while black carbon (BC) showed slight increases, and in some cases, even decreases (Manoj et al., 2019; McDuffie et al., 2020). In China, Air Pollution Prevention and Control Action Plan was implemented in 2013 to address severe air pollution, resulting in emissions reductions of aerosols and their precursors (Gao et al., 2022; Zheng et al., 2018). Near-surface $PM_{2.5}$ (particulate matter with a diameter less than 2.5 μm) concentrations in China decreased by approximately 33.3% from 2013 to 2017, indicated in ground-based measurements (Huang et al., 2018).

Anthropogenic emissions are a major source of atmospheric aerosols. In addition, wildfires, including human-made fires (Syphard et al., 2007), naturally occurring fires such as those from lightning (Larjavaara et al., 2005), and agricultural waste burning (Cheng et al., 2009), also contribute significantly to aerosols. Wildfire is a natural part of many ecosystems, and its frequency and intensity are influenced by a variety of meteorological factors (Tomshin & Solovyev, 2022; Zacharakis & Tsihrintzis, 2023). Key factors affecting wildfire occurrence include temperature, precipitation, wind patterns, and humidity levels (Richardson et al., 2022). Elevated temperatures and prolonged dry periods create conditions that are conducive to wildfires by drying out vegetation and making it more flammable. Additionally, wind can exacerbate wildfire spread by providing more oxygen and carrying embers to new areas, while low humidity levels reduce the moisture content in vegetation, further increasing fire risk. Siberia is highly fire-prone (Pan et al., 2020; Ponomarev et al., 2023) and has experienced the greatest warming in the Eastern Hemisphere during the past few decades (Petäjä et al., 2021). Eastern Siberia exhibited a positive trend in surface air temperature and a negative trend in precipitation during 2001–2020 (Tomshin & Solovyev, 2022). Luo et al. (2024) reported that approximately 79% of the increase in vapor pressure deficit (VPD) over eastern Siberia, which controls wildfire activity, was driven by summer Russian Arctic sea-ice decline, whereas the remaining 21% was attributed to internal atmospheric variability related to Siberian blocking events during 2004–2021. All these changes led to an increase in burned area (Tomshin & Solovyev, 2022; Xing & Wang, 2023) and a rising trend in biomass burning aerosol emissions in Siberia during 2001–2020 (Chen et al., 2023). Under continued Arctic warming, Siberian wildfires are likely to increase in the future (Gui et al., 2024; Huang et al., 2024).

Arctic warming is largely driven by both local forcing and feedbacks, as well as by remote forcings through poleward energy transport from lower latitudes (Alexeev et al., 2005; Graversen & Langen, 2019; Ren et al., 2020; Semmler et al., 2020; Stuecker et al., 2018; Yang et al., 2018). GHGs, which are homogeneously distributed and have been steadily increasing since preindustrial times (Friedlingstein et al., 2023; IPCC, 2013, 2021), and aerosols, which are highly regional and exhibit varying change patterns across regions (Gao et al., 2022, 2023; Hoesly et al., 2018; Li et al., 2017; Samset et al., 2019; Tomshin & Solovyev, 2022), are among the most significant anthropogenic climate forcers affecting both global and Arctic warming (Stjern et al., 2019). Arctic warming driven by GHGs has been extensively investigated before (Dai et al., 2019; Liang et al., 2022; Zhou et al., 2023). A recent study by Wu et al. (2024) reported that anthropogenic aerosols were more efficiently in contributing to Arctic amplification compared to GHGs, due to the greater sensitivity of Arctic sea ice and the resulting changes in ocean-atmosphere heat exchange in response to aerosol forcing. However, the Arctic climate responses to regional aerosol perturbations, particularly the recent rapid evolution of aerosols (Gao et al., 2023) and the likelihood of further changes in their patterns in the future (Samset et al., 2019; Wang et al., 2023) remain less understood (Sand et al., 2016).

Given that emissions of aerosol and precursors in the Northern Hemisphere have experienced rapid changes during the past few decades, it is necessary to quantify the Arctic responses to such regional biomass burning/anthropogenic emissions of aerosols and precursors. This study aims to evaluate the changes in aerosols and their precursors resulting from human activities and wildfires in the key polluted/burning areas of Northern Hemisphere (e.g., China, SA, North America, Europe, and Siberia) during the period 2013–2019 and investigate climate responses in the Arctic to these regional aerosol changes using the Community Earth System Model version 1 (CESM1).

2. Methods

2.1. Observational Data and Meteorological Reanalysis

AOD data are acquired from the Moderate Resolution Imaging Spectroradiometer (MODIS) Deep Blue product, which offers detailed information on aerosol optical properties (Hsu et al., 2013a, 2013b). The AOD data are used to evaluate aerosol changes across regions and validate the performance of CESM1 in capturing aerosol trends and patterns.

ERA5 is a global atmospheric reanalysis data set produced by the European Centre for Medium-Range Weather Forecasts (ECMWF), providing a comprehensive view of the earth's atmosphere from 1940 to near real-time (Hersbach et al., 2020a, 2020b). Monthly data of surface solar radiation, 2-m air temperature, total precipitation, relative humidity, and zonal components of winds are obtained from the ERA5 reanalysis to assess the favorable climate conditions for wildfires and the increase in associated wildfire risks in Siberia. Wildfire risk indices used in this study include reference potential evapotranspiration (ET_0), VPD, and McArthur forest fire danger index (FFDI), which were widely applied to represent wildfire risks (e.g., Ren et al., 2022 and references therein).

2.2. Model Description, Emission, and Experimental Design

CESM1 (Hurrell et al., 2013) is used in this study to investigate the climatic impacts of aerosols. CESM1 is a globally coupled climate model consisting of multiple components representing the atmosphere, ocean, land surface, sea ice etc. By integrating these earth system components, the coupled CESM1 effectively simulates complex interactions among the atmosphere, ocean, land, and sea ice, providing a comprehensive understanding of the climate system. The Community Atmosphere Model version 5 (CAM5) within CESM1 is responsible for simulating atmospheric physical and chemical processes, with the default horizontal resolution of 1.9° latitude by 2.5° longitude and 30 vertical layers. The model version in this study incorporates the four-mode version of the Modal Aerosol Module (MAM4) (Liu et al., 2016), which predicts various aerosol species, including sulfate, BC, primary organic matter (POM), secondary organic aerosol (SOA), mineral dust, and sea salt, distributed across four lognormal modes (Aitken, accumulation, coarse, and primary carbon modes). The Community Ice CodE (CICE) module within CESM1 is dedicated to modeling the dynamic and thermodynamic processes of sea ice, and the Parallel Ocean Program (POP) is used for modeling global ocean dynamics.

Biomass burning emissions of aerosols and precursors are from Global Fire Emissions Database version 4.1s (GFED 4.1s) (Van Der Werf et al., 2017). The global anthropogenic emissions of aerosols and their precursors are provided by the Community Emissions Data System (CEDS), specifically version 2021_04_21. Biogenic emissions derived from Model of Emissions of Gases and Aerosols from Nature version 2.1 (MEGAN 2.1) (Guenther et al., 2012) are fixed at year-2013 levels globally in all experiments.

This study aims to quantify the impacts of changes in regional anthropogenic/biomass burning aerosols on the Arctic climate from 2013 to 2019. We conduct a series of fully coupled model experiments using CESM1, as detailed in Table 1:

1. BASE: A baseline experiment using the fully coupled model configuration, where anthropogenic and biomass burning emissions of aerosols and precursors are fixed at year-2013 levels globally.
2. CN: Similar to BASE, but with anthropogenic emissions of aerosols and precursors over China fixed at year-2019 levels.
3. CN + SI: Similar to CN, but with biomass burning emissions of aerosols and precursors over Siberia adjusted to include 2013–2019 emission trends. Specifically, a linear trend of biomass burning emissions during 2013–2019 is calculated at each model grid over Siberia. This trend is then multiplied by six (corresponding to the

Table 1
Experimental Design

Experiments	Year of input for emissions of aerosols and precursors			
	CN (ANT)	SA (ANT)	NA + EU (ANT)	SI (BB)
BASE	2013	2013	2013	2013
CN	2019	2013	2013	2013
CN + SI	2019	2013	2013	2013 + (2013–2019 trends)
CN + SI + SA	2019	2019	2013	2013 + (2013–2019 trends)
NA + EU	2013	2013	2019	2013

Note. CN/SA/SI/NA/EU represents China/South Asia/Siberia/North America/Europe. ANT/BB represents anthropogenic/biomass burning emissions.

6-year difference from 2013 to 2019) and added to the 2013 baseline emissions at each grid to roughly minimize the potential influence from interannual variability.

4. CN + SI + SA: Similar to CN + SI, but with anthropogenic emissions of aerosols and precursors over SA fixed at year-2019 levels.
5. NA + EU: Similar to BASE, but with anthropogenic emissions of aerosols and precursors over North America and Europe fixed at year-2019 levels.

The differences between each pair of these fully coupled simulations illustrate the climate responses to emissions changes. Specifically, the differences between BASE and CN, as well as between BASE and NA + EU, isolate the climate responses to changes in anthropogenic emissions of aerosols and precursors originating from China and from North America and Europe, respectively, during 2013–2019. The differences between CN and CN + SI reflect the climate responses to changes in biomass burning emissions over Siberia, while the differences between CN + SI and CN + SI + SA capture the additional effects of changes in anthropogenic emissions from SA. Each fully coupled simulation is conducted for at least 150 years, with the final 100 years used for analysis. To reduce model noise, three ensemble simulations are conducted for each experiment by applying small temperature perturbations to the initial atmospheric conditions.

Aerosol radiative effect (ARE) is calculated as the net change in radiative flux at the top of the atmosphere (TOA) between the perturbed and control simulations induced by aerosol changes. Positive values indicate a net energy gain of the climate system, while negative values indicate energy loss.

In addition, to assess the robustness of the simulated climate responses, the magnitude of the responses in each sensitivity experiment is compared with the range of internal variability estimated from long-term preindustrial control simulations of the CESM1 Large Ensemble Community Project (LENS). The preindustrial control simulations, which are performed under constant preindustrial forcing conditions, provide a baseline estimate of the model's natural variability in the absence of external forcing. By comparing the simulated responses with this internal variability range, it is possible to determine whether the aerosol-induced climate signals exceed the level of internal noise and can therefore be regarded as statistically robust.

2.3. Northward Heat Transport Calculation

At each latitude, the northward heat transport (NHT) (Hwang et al., 2011) is obtained by integrating the energy imbalance over the spherical cap from the pole to that latitude:

$$\mathrm{NHT}(\phi) = 2\pi a^2 \int_{-\frac{\pi}{2}}^{\phi} R(\phi') \cos \phi' d\phi'$$

where NHT (ϕ) is the NHT across latitude ϕ, a is the Earth's radius, and $R(\phi')$ is the zonal-mean energy imbalance at latitude ϕ'. ϕ' indicates the intermediate latitudes over which the integration is performed, from the South Pole up to latitude ϕ.

10.1029/2025EF007516

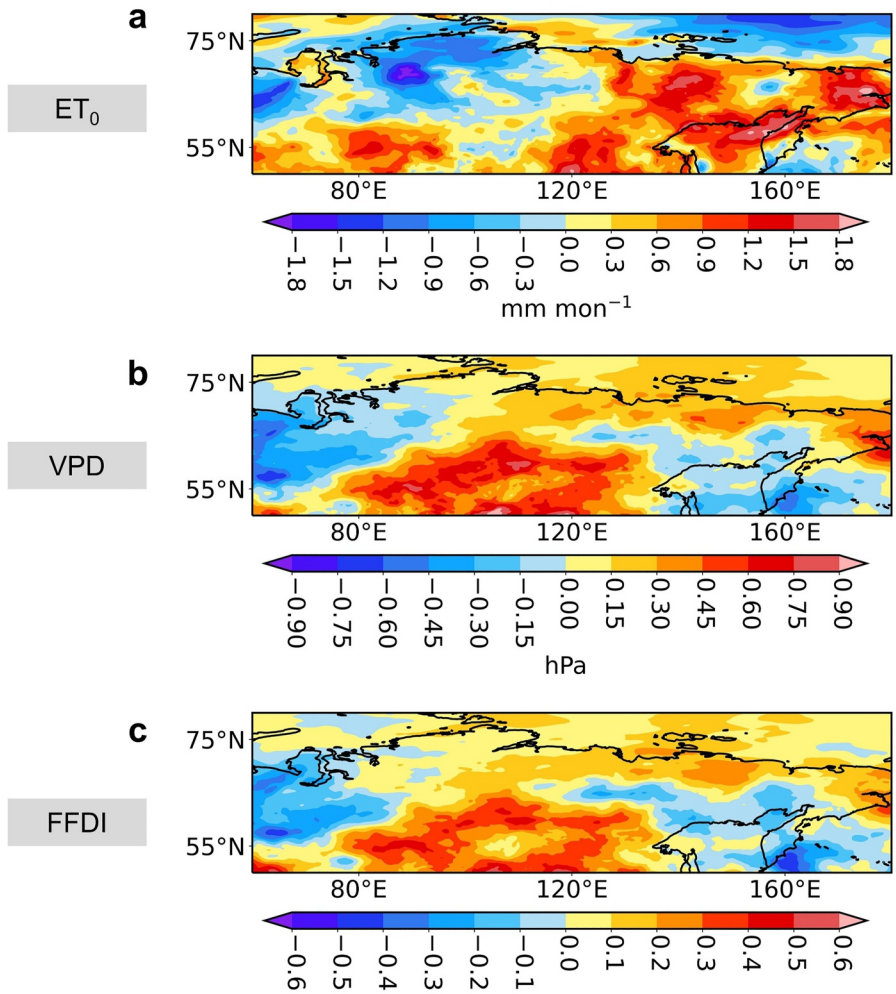

Figure 1. Spatial distributions of absolute differences in wildfire risk indices, including (a) reference potential evapotranspiration (ET_0, unit: mm mon^{-1}), (b) vapor pressure deficit (VPD, unit: hPa), and (c) McArthur forest fire danger index (FFDI, unitless) over Siberia between 2011–2013 and 2017–2019 (2017–2019 minus 2011–2013) from ERA5 reanalysis.

The NHT is diagnosed separately for the atmosphere (including both dry static and moisture components), the ocean, and the total climate system. The total NHT is derived from the net top-of-atmosphere (TOA) radiative flux imbalance. The oceanic NHT is calculated from sea surface heat flux imbalance. The atmospheric NHT is then obtained as the residual.

3. Results

3.1. Rising Wildfire Occurrence and Related Emissions in Siberia

Siberia, known for its vast forests and harsh climate conditions, has experienced significant climate changes. Several areas of Eastern Siberia have experienced rising temperatures, reduced humidity and precipitation, and increased wind speeds (Figure S1 in Supporting Information S1), all of which have contributed to the growth of wildfires in the region during 2013–2019. This is shown in Figure 1 and Figure S2 in Supporting Information S1, with increases in wildfire risk indices in many parts of Siberia. The three indices exhibit distinct spatial variations due to their different sensitivities to specific climate variables. For example, ET_0 increased the most over Russian Far East, while VPD and FFDI have the largest increases over 80°–120°E of Siberia. The observed increase in Siberian wildfire aerosols during 2013–2019 reflects not only short-term variability but also a broader long-term

10.1029/2025EF007516

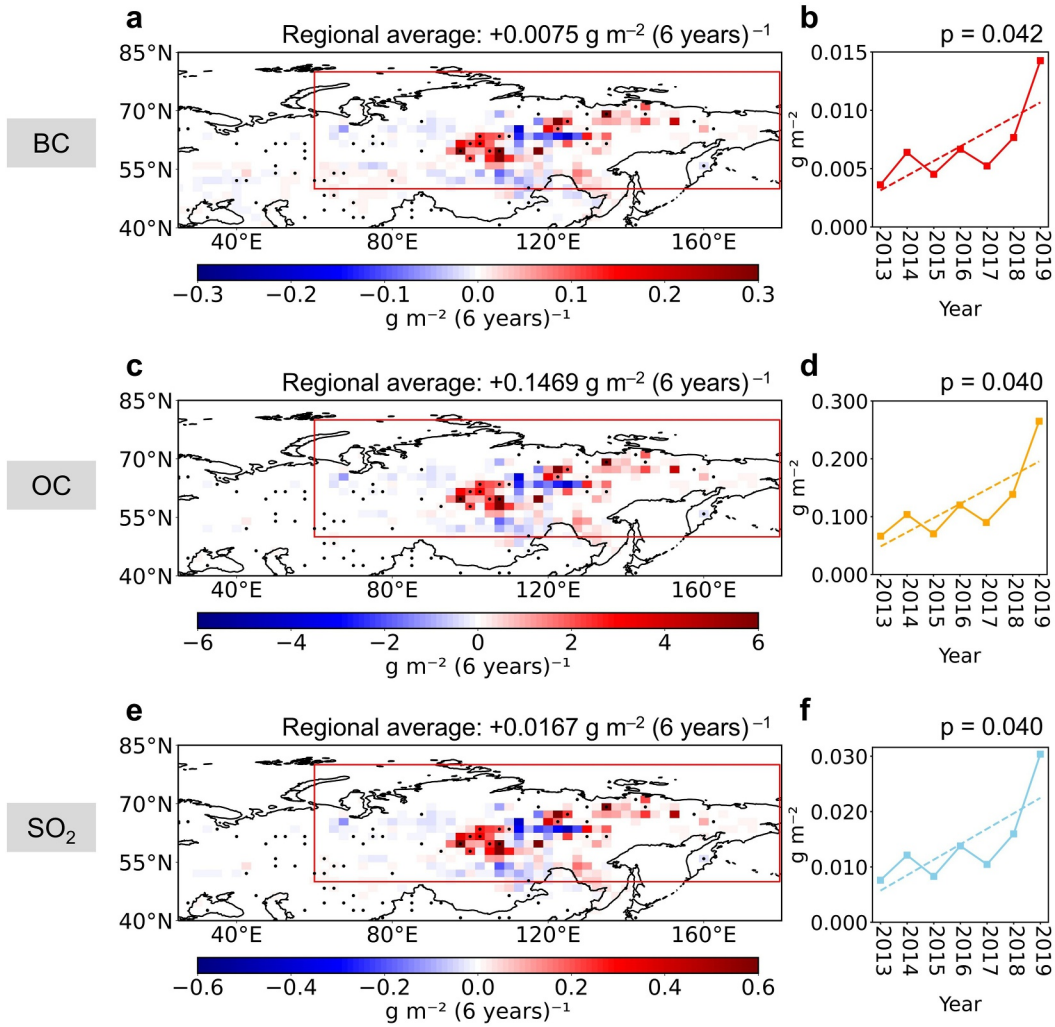

Figure 2. (a, c, and e) Spatial distributions and (b, d, and f) time series of biomass burning emissions (unit: g m^{-2}) of aerosols and precursors over Siberia, including (a and b) black carbon, (c and d) organic carbon and (e and f) sulfur dioxide (SO_2). Areas with p value of trends <0.1 are marked with black dots. Regional averages over continental grids within the red box and p values of linear trends are noted at the top of the panels.

trend. Several studies have reported a sustained rise in wildfire activity across boreal regions since the early 2000s (Zheng et al., 2023; Zhong et al., 2024).

Wildfire occurrence in Siberia has led to the corresponding biomass burning emissions of aerosols and precursors. Wildfires release a variety of aerosols and precursors, including BC, organic carbon (OC), and other particulate matter, which have significant implications for climate and air quality. GFED emission data show overall increasing trends of biomass burring emissions of BC, OC and SO_2 over Siberia from 2013 to 2019 (Figure 2). Considering the uneven increasing trend of biomass burning emissions in Siberia (Figure 2), along with significant year-to-year fluctuations, in the related CESM1 equilibrium simulations, biomass burning emissions are either fixed at the 2013 level or adjusted to include the trends from 2013 to 2019 without taking the interannual variability into account (Table 1). This method takes into account high interannual variability in fire emissions when compared to directly using biomass burning emissions at 2013 and 2019 levels for equilibrium simulations. Figure S3 in Supporting Information S1 illustrates biomass burning emissions of aerosols and precursors over Siberia as input to the CESM1 simulations and their differences, also highlighting the increase in biomass burning aerosols from Siberian wildfires during this period as captured by the simulations. Siberian wildfire emissions exhibit a pronounced increases in boreal summer and a weaker increase in boreal spring and autumn (Figure S4 in Supporting Information S1). This seasonality is consistent with the climatological background over Siberia,

10.1029/2025EF007516

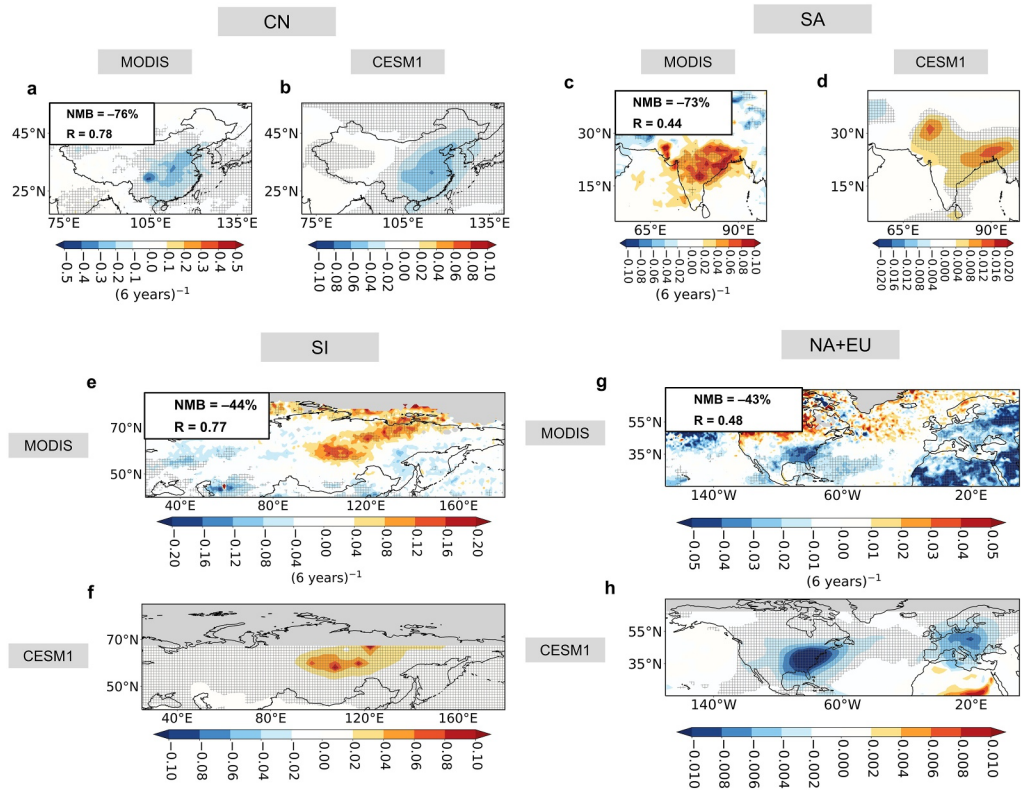

Figure 3. Spatial distributions of changes in annual mean AOD from (a, c, e, and g) MODIS retrievals (linear trends) and (b, d, f, and h) CESM1 simulations (differences (b) between simulations BASE and CN, (d) between simulations CN + SI and CN + SI + South Asia (SA), (f) between simulations CN and CN + SI, and (h) between simulations BASE and NA + EU) over (a and b) China (CN), (c and d) SA, (e and f) Siberia (SI), and (g and h) North America-Europe (NA + EU). Normalized mean bias (NMB) and correlation coefficient (R) between modeled AOD and MODIS AOD are shown at the upper-left corner of panel (a, d, e, and g). NMB = $100\% \times \sum$ (AOD-CESM1$_i$ − AOD-MODIS$_i$)/$\sum$ AOD-MODIS$_i$, where AOD-CESM1$_i$ and AOD-MODIS$_i$ are the CESM1-modeled and MODIS AOD values at grid i, respectively. The shaded areas indicate results are statistically significant at the 90% confidence level. Missing values are shown in gray.

where warm and dry summer conditions, combined with frequent lightning activity, enhance wildfire occurrence and associated emissions.

The ability of CESM1 to capture observed aerosol changes is assessed by comparing the modeled responses in AOD to regional emission perturbations with the overall AOD trends retrieved from MODIS (Figure 3). It should be noted that MODIS reflects the total AOD changes during 2013–2019 from all aerosol species and all source regions, whereas the CESM1 perturbation experiments isolate the AOD contribution associated with emissions from a specific region (e.g., Siberia only). In Siberia, both MODIS and CESM1 indicate an increasing trend in aerosols associated with wildfire activity (Figures 3a and 3b). The simulations modeled by increased wildfire aerosol emissions systematically underestimates the magnitude of the observed AOD trend, with a normalized mean bias (NMB) of −44%. Similarly, the underestimate of AOD magnitude by CESM has been reported in many previous studies (Gao, 2025; Gao et al., 2022, 2023; Ren et al., 2022). However, given the high forcing sensitivity to aerosols in CESM (Gettelman et al., 2019), the underestimation in magnitude is unlikely to substantially affect the simulated climate responses in this study.

3.2. Changes in Anthropogenic Aerosols From China, South Asia, North America, and Europe

Since 2013, China has reduced aerosol emissions significantly, with BC, OC, and SO_2 decreasing by 0.031, 0.022, and 1.301 g m^{-1}, respectively (Figure S5 in Supporting Information S1). In SA, SO_2 increased by 0.365 g m^{-1}, while BC and OC decreased (Figure S6 in Supporting Information S1). Similarly, emissions in Europe and North America have dropped since the 1970–1980s, with BC, OC, and SO_2 decreasing by 0.004 g m^{-1}, 0.007 g m^{-1}, and 0.126 g m^{-1}, respectively, from 2013 to 2019 (Figure S7 in Supporting Information S1). Anthropogenic

10.1029/2025EF007516

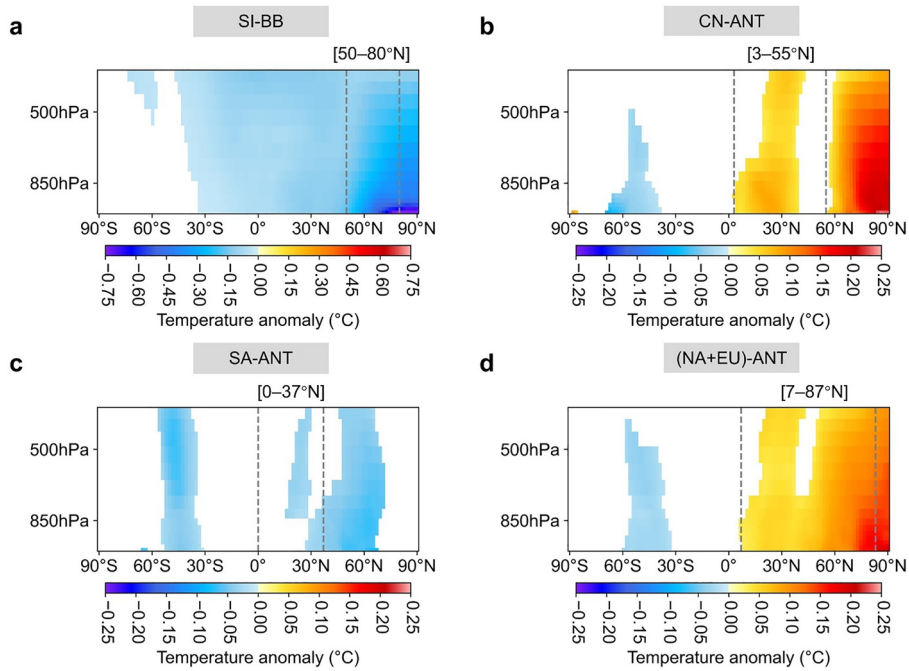

Figure 4. Vertical profile of simulated zonal-mean responses in air temperature (unit: °C) to changes in anthropogenic/biomass burning (ANT/BB) emissions of aerosols and precursors from individual regions, including (a) Siberia (SI), (b) China (CN), (c) South Asia (SA), and (d) North America and Europe (NA + EU). The vertical dashed lines mark the latitude ranges of SI, CN, SA, and NA + EU, respectively, in the corresponding panel. Areas with statistical significance below the 90% confidence level are masked.

emissions over China, SA, and North America-Europe do display an obvious changes during 2013–2019, with relative strong decreases in boreal winter (December–February, Figures S8–S10 in Supporting Information S1) driven by large energy demand during the cold season.

For regional AOD changes between 2013 and 2019, MODIS satellite retrieval reveals distinct aerosol trends that a marked decline in AOD over China, a moderate decline in Europe and North America, and an increase over SA (Figure 3). These aerosol perturbation simulations underestimate the magnitude of observed AOD changes over China, North America-Europe, and SA (NMB = −76%, −73%, −43%). This systematic low bias is consistent with findings from earlier CESM1 studies and has also been widely reported in other CMIP6 models (Gliß et al., 2021; He et al., 2015; Ren et al., 2024; Tsigaridis et al., 2014; Turnock et al., 2020). The magnitude of aerosol underestimation in CESM is comparable to, or slightly exceeds, that in other CMIP6 models.

3.3. Arctic Climate Responses to Regional Anthropogenic and Wildfire Aerosol Changes

Figure 4 illustrates the vertical profiles of the zonal-mean air temperature response to changes in aerosols and their precursors originating from individual regions. Changes in aerosols from individual regions significantly influence air temperature within the corresponding latitude bands. For instance, the increase in aerosol over Siberia results in noticeable cooling within the specific latitude range of 50°–80°N. Similarly, the slight increase in aerosols in SA leads to marginal cooling, whereas reductions in aerosol emissions from China, Europe, and North America are associated with warming within their respective latitude bands during 2013–2019. It is also indicated by the spatial distribution of surface air temperature differences between the baseline and sensitivity runs (Figure S11 in Supporting Information S1). Notably, air temperatures in the Arctic are significantly affected by aerosol changes occurring at lower latitudes and the influences are even more pronounced than those observed in the local latitude bands where the aerosol perturbations originate, manifesting an amplified Arctic warming (Figure 4).

Changes in aerosols, clouds, and circulation fields have been examined (Figures S12–S14 in Supporting Information S1). The largest perturbations in aerosol concentrations are found within their respective source latitude bands (Figure S12 in Supporting Information S1), in agreement with the emission changes imposed. Increased

10.1029/2025EF007516

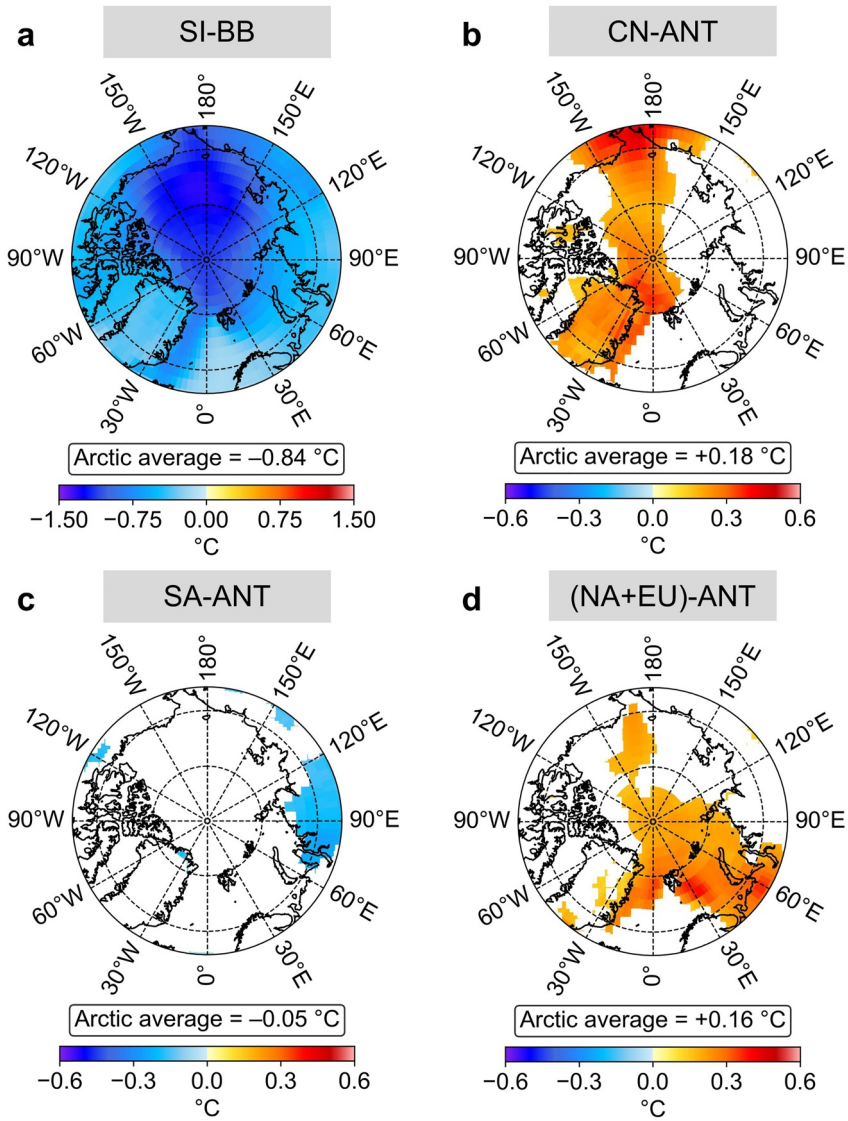

Figure 5. Spatial distributions of simulated Arctic responses in surface air temperature (unit: °C) to changes in anthropogenic/biomass burning (ANT/BB) emissions of aerosols and precursors from individual regions, including (a) Siberia (SI), (b) China (CN), (c) South Asia, and (d) North America and Europe (NA + EU). Areas with statistical significance below the 90% confidence level are masked.

aerosols over Siberia are found to influence cloud amount over the Arctic (Figure S13a in Supporting Information S1). This effect may involve both aerosol–cloud microphysical interactions and large-scale dynamical adjustments. However, it cannot be clearly determined which of these processes exerts the dominant influence and requires further investigation. Aerosol perturbations from other regions are found to have comparatively much weaker effects on Arctic cloud amount (Figures S13b–S13d in Supporting Information S1), indicating that the Siberian emissions play a uniquely important role in modulating cloud at high latitudes. Circulation changes are weak, but a tendency of shift in near-surface winds in the equatorial due to the hemisphere temperature gradient change is detected (Figure S14 in Supporting Information S1).

Increased wildfire aerosol emissions from Siberia have resulted in a 0.84°C cooling in the Arctic (north of 66.5°N) during 2013–2019 (Figure 5a). In contrast, due to clean air actions, aerosol reductions in China, Europe-North America have caused Arctic warming of 0.18°C and 0.16°C, respectively (Figures 5b and 5d). The cooling due to increase in aerosols from Siberian wildfires overwhelms the potential warming caused by aerosol reductions in China, Europe, and North America. The net cooling related to such aerosol changes has partly offset

10.1029/2025EF007516

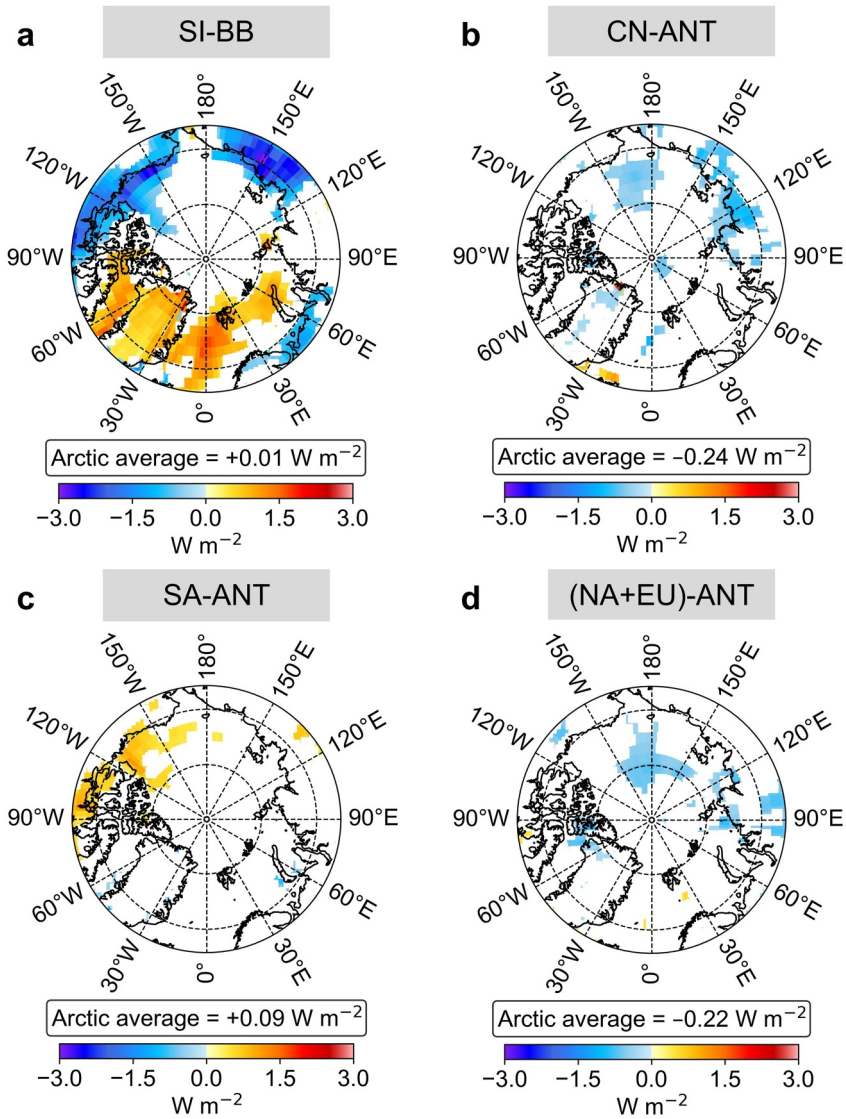

Figure 6. Spatial distributions of simulated Arctic responses in Aerosol radiative effect (unit: W m^{-2}) to changes in anthropogenic/biomass burning (ANT/BB) emissions of aerosols and precursors from individual regions, including (a) Siberia (SI), (b) China (CN), (c) South Asia, and (d) North America and Europe (NA + EU). Areas with statistical significance below the 90% confidence level are masked.

the recent strong Arctic warming induced by GHGs. The temperature impact on the Arctic from emission changes in SA is relatively small, with only a 0.05°C cooling in the Arctic (Figure 5c). The relatively small impact of SA's emission changes on Arctic temperatures, compared to other emitting regions, is primarily due to differences in geographic separation to the Arctic, changes in large-scale circulation patterns, surface albedo feedback, cloud feedback, and the Coriolis effect associated with their respective locations (Dagan et al., 2021; Persad & Caldeira, 2018; Persad et al., 2023; Williams et al., 2023). The changes in snow/ice surface temperatures mirror the changes in surface air temperatures (Figure S15 in Supporting Information S1). Accompanying these Arctic temperature changes are shifts in Arctic ice and snow amount (Figures S16–S19 in Supporting Information S1). The increase in aerosols from Siberia has led to more Arctic ice and snow. In contrast, the reduction in emissions from China, Europe, and North America has contributed to a reduction of Arctic ice and snow. The overall albedo of Arctic snow and ice changes in parallel with their amount (Figure S20 in Supporting Information S1).

Changes in radiative forcing (Figure 6) and surface air temperature (Figure 5) in the Arctic do not show a strong correlation and even exhibit opposite variation. In the case of the responses to aerosol reductions in China, the

10.1029/2025EF007516

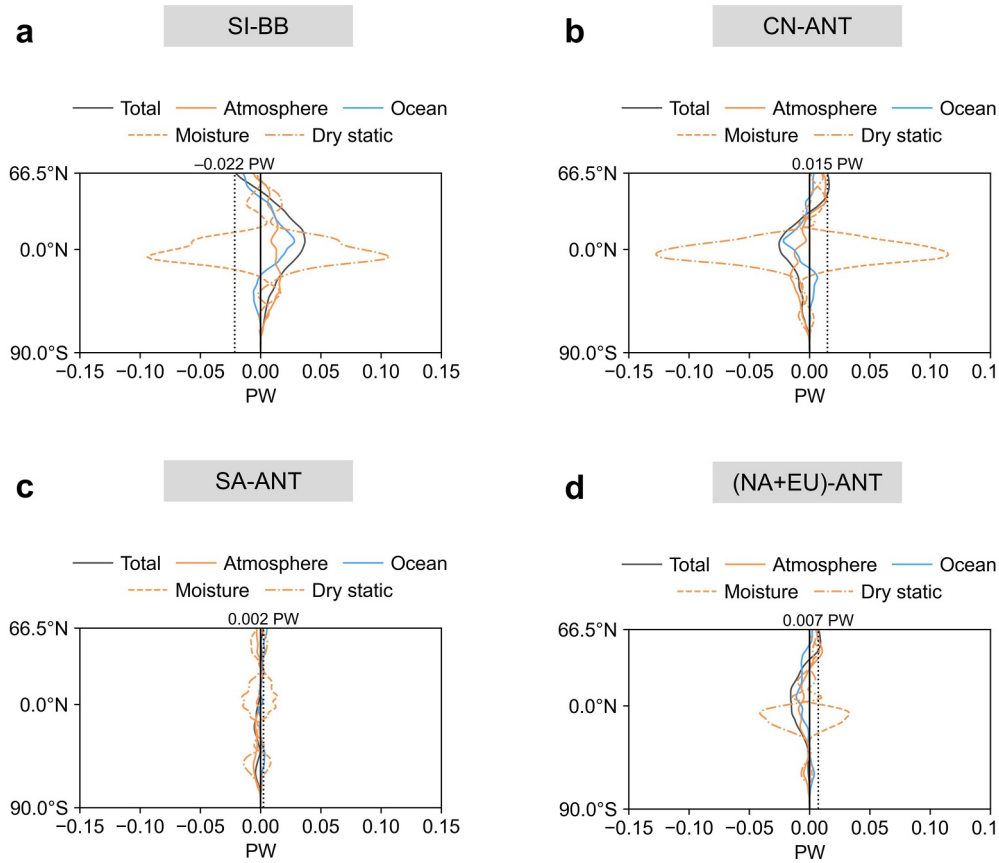

Figure 7. Simulated zonal mean responses in annual mean northward heat transport (NHT) (unit: PW) in the atmosphere (blue dashed lines), oceans (red dashed lines) and both of them combined (black solid lines) to changes in anthropogenic/biomass burning (ANT/BB) emissions of aerosols and precursors from individual regions, including (a) Siberia (SI), (b) China (CN), (c) South Asia, and (d) North America and Europe (NA + EU). The NHT in the atmosphere is also divided into moisture and dry static components. The NHT near the Arctic Circle (approximately 66.5°N) is highlighted in each figure.

Arctic's local radiative forcing changes are negative (Figure 6b), but the temperature changes are positive (Figure 5b), suggesting that the local RF changes induced by the remote aerosols are not the major factor causing the temperature changes in the Arctic. The NHT near the Arctic Circle (about 66.5°N) shows a signal consistent with the temperature changes in the Arctic (Figure 7). Aerosol reductions in China and Europe-North America led to a positive NHT across the Arctic Circle (Figures 7b and 7d), while the increase in Siberian wildfire emissions caused a negative NHT across the Arctic Circle (Figure 7a). It indicates that the response of NHT to aerosol changes over distant regions outside the Arctic, rather than the local radiative effect, drives the Arctic temperature changes. For the Siberian aerosol perturbation, the changes in NHT near the Arctic circle are dominated by the oceanic component, as simulated by CESM1 (Figure 7a). In contrast, the NHT anomalies induced by aerosol reductions over China and North America–Europe are attributed to atmospheric processes, within which the dry static energy component contributes more substantially than the moisture component (Figures 7b and 7d). In our study, NHT is primarily influenced by ARE originating outside the Arctic Circle. Such ARE changes may result from the direct radiative effects of aerosols, aerosol–cloud interactions, and various other feedback processes. Due to the limitations of the current model configuration, however, the relative contributions of these processes cannot be quantitatively diagnosed. Overall, the ARE induced by Siberian biomass burning aerosols is negative outside the Arctic Circle, whereas the ARE associated with anthropogenic aerosol reductions over China and North America–Europe is positive (Figure S21 in Supporting Information S1). These ARE anomalies exhibit the same sign compared with the corresponding anomalies in NHT across the Arctic Circle (Figure 7).

10.1029/2025EF007516

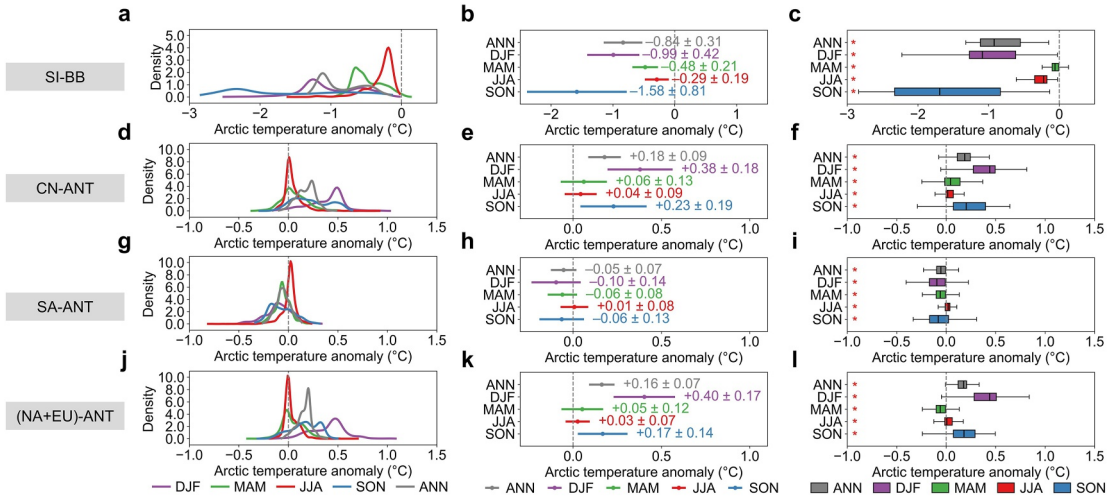

Figure 8. (a, d, g, and j) Probability density functions, (b, e, h, and k) range bars, and (c, f, i, and l) box plots of simulated Arctic seasonal responses in surface air temperature (unit: °C) to changes in anthropogenic/biomass burning (ANT/BB) emissions of aerosol and precursors from individual regions, including (a, b, and c) Siberia (SI), (d, e, and f) China (CN), (g, h, and i) South Asia, and (j, k, and l) North America and Europe (NA + EU). The range bars in panels b, e, h, and k represent one standard deviation. The red asterisks in panels c, f, i, and l indicate the responses are significant based on K–S test ($p < 0.05$).

The responses in Arctic surface air temperature to regional anthropogenic aerosol changes exhibit clear seasonal variations, with the strongest warming occurring in winter (DJF), followed by autumn (SON), spring (MAM), and summer (JJA) (Figure 8). Two sea-ice-related climate feedbacks are particularly relevant: (a) the ice-albedo feedback during summer, involving the intraseasonal storage and release of energy, and, (b) wintertime sea ice-infrared radiation feedbacks, influenced by changes in clouds, inversion strength, and moisture content (Bintanja & Van Der Linden, 2013). Such a winter-dominated warming pattern aligns with previous studies, which reported enhanced Arctic warming in winter compared to summer (Bintanja & Van Der Linden, 2013; Serreze et al., 2009; Serreze & Francis, 2006). This seasonal temperature response can also be explained by the changes in seasonal anthropogenic emissions, particularly the decrease in SO_2 emissions, which follow a general seasonal pattern of DJF > SON > MAM > JJA (Figures S8–S10 in Supporting Information S1). However, the Arctic temperature responses to aerosol increases from Siberian wildfires deviate slightly from this general pattern, showing a peak in SON rather than in DJF (SON > DJF > MAM > JJA). Stronger cooling in SON than in DJF is due to much more emission increases in SON than in DJF. Specifically, OC from Siberian wildfires increased markedly in SON (0.58 mg m^{-2}), whereas in DJF, OC levels remained unchanged or even slightly declined (−0.07 mg m^{-2}) (Figure S4 in Supporting Information S1).

4. Conclusions and Discussions

This study quantifies the climate responses in the Arctic to changes in anthropogenic or biomass burning emissions of aerosols and their precursors from key regions in the Northern Hemisphere: China, SA, Europe, North America, and Siberia, during 2013–2019 using the CESM1 model. During 2013–2019, notable changes in global aerosols and their precursors were observed. In China, Europe, and North America, clean air actions led to a reduction of anthropogenic aerosols. Conversely, Siberia experienced an increase in wildfire aerosols due to the local warmer and drier conditions. In SA, the emission changes varied by aerosol species, with a significant increase in SO_2 and a slight decrease in carbonaceous aerosols. Changes in regional aerosols not only exert influence on temperatures within their respective latitude bands but also significantly impact Arctic temperatures. The reduction in aerosols from China and Europe-North America contributes to a near-surface warming effect of +0.18°C and +0.16°C, respectively, over the Arctic. Changes in anthropogenic emissions from SA have a negligible impact on the Arctic climate. Within the overall context of reductions in anthropogenic aerosols, it is noteworthy that the increase in aerosols from Siberian wildfires leads to an Arctic cooling effect by −0.84°C. The Arctic temperature responses are found to be predominantly governed by changes in NHT induced by aerosol changes in lower latitudes, rather than by local radiative effects. The cooling owing to the increased aerosols from Siberian wildfires overwhelms the potential warming caused by aerosol reductions in China, Europe, and North

America. The Arctic ice and snow amount exhibit nearly opposite changes to temperature changes in the Arctic. Additionally, a significant seasonal variation in these Arctic climate responses to aerosol perturbations, with a stronger (weaker) response in boreal winter (summer), is also identified. The seasonal response to Siberian wildfires is different, given that the wildfire emissions peak in boreal autumn.

The results in this study are to some extent different from Zhong et al. (2024), which reported that a rise in boreal biomass burning aerosol emissions resulted in positive local radiative effects during Arctic summer, leading to the Arctic warming. The different findings can be attributed to the following factors. First and foremost, while Zhong et al. (2024) focused exclusively on local radiative effects, our study emphasizes the temperature changes influenced by both local radiative effects and meridional energy transport and the latter is found to dominate Arctic temperature changes in response to the remote aerosol changes. Second, the methodological differences in model configuration can contribute to the discrepancy. Zhong et al. (2024) used an atmosphere-only model, whereas our study is based on a fully coupled model, allowing for ocean-atmosphere interactions that potentially change the response of different system components. Third, the aerosol species considered differ between studies. While Zhong et al. (2024) focused solely on carbonaceous aerosols, our investigation additionally accounts for sulfate aerosols. The enhanced cooling effect of additional sulfate aerosols can also contribute to the Arctic cooling.

Zheng et al. (2023) reported that under the amplified Arctic warming, wildfires in regions like Siberia were expected to increase, thereby diminishing carbon sink capabilities and exacerbating Arctic warming. This creates a positive feedback mechanism between Arctic warming and Siberian wildfires. Siberia wildfires emit a large amount of CO_2, further enhancing the global and Arctic warming (Liu et al., 2014), which is another positive feedback mechanism between Arctic warming and Siberian wildfires. Our study introduces a feedback mechanism from the perspective of aerosols: with the intensified warming in the Arctic Siberia, wildfires in Siberia lead to increased aerosol emissions, resulting in a cooling effect on the Arctic. This forms a negative feedback mechanism between Arctic warming and Siberian wildfires.

Figure S22 in Supporting Information S1 shows the impact of aerosol changes across different regions on Arctic temperatures in our study and the estimated Arctic temperature changes attributed to CO_2 concentration increases from 2013 to 2019, roughly calculated using the global temperature sensitivity to CO_2 changes from IPCC (2021) and the Arctic amplification ratio of 4 reported by Rantanen et al. (2022), as well as the Arctic temperature changes from 2013 to 2019 from ERA5 reanalysis. Based on ERA5 data, the Arctic surface air temperature change is estimated at +1.04°C, comparable to the estimated Arctic surface air temperature change (+0.42 to +1.05°C) based on changes in CO_2 concentrations during this period. The surface cooling induced by the increase in aerosols from Siberian wildfires is partly offset by the warming effect from the reductions in anthropogenic aerosols. It should be noted that the temperature responses presented in this study are derived from equilibrium experiments, which assume a fully adjusted climate system to the imposed forcing. The Arctic's transient response to aerosol perturbations may be slower and weaker, suggesting that the near-term climate effects of increased Siberian wildfire aerosols could be overestimated in equilibrium simulations. Internal climate variability (Chen & Dai, 2024; Sweeney et al., 2023) and the effects of other GHGs were not considered in this estimation, which may have also influenced the Arctic climate changes.

Internal variability is a well-established driver of Arctic climate change (Chen & Dai, 2024; Swart et al., 2015) and could potentially influence the robustness of our results. Probability density function of the CESM1 preindustrial control simulations, which include no external forcing, shows that Arctic surface temperature varies between approximately −12°C and −16°C across different model years, indicating a spread of ∼4°C (Figure S23 in Supporting Information S1). This large range clearly demonstrates the substantial internal variability of Arctic temperatures, highlighting that internal variability can contribute significantly to Arctic climate changes and must be considered when interpreting aerosol-forced temperature responses. However, our estimated temperature responses are based on three ensemble members, each covering 100 years. Thus, the reported responses represent the differences between two 300-year climatological means. Such long-term averaging already removes most of the year-to-year internal variability. In other words, the forced signals we report have largely been separated from internal noise. We also conducted additional statistical tests. The K-S test indicates that Arctic temperature responses under the individual aerosol perturbation experiments are statistically significant (Figure 8c, 8f, 8i, and 8l). Therefore, the reported signal has already been averaged over hundreds year simulations to filter out noise and remains statistically significant. The conclusions are thus robust.

Continued Arctic warming may create increasingly favorable conditions for wildfire activity in Siberia, increasing both the frequency and intensity of wildfires in this region. As a result, wildfire-related aerosol emissions could become a more prominent component of the Arctic climate system, potentially reinforcing the negative feedback mechanism identified in this study. However, this feedback is associated with adverse effects such as ecosystem degradation, air quality deterioration, and carbon release, and should not be regarded as a sustainable or desirable climate regulation process. Future Earth system models and climate policies should account for these evolving wildfire-aerosol-climate interactions to better understand the implications of a warming Arctic.

Our study has some uncertainties and requires further investigation. First, the results are based on a single climate model, which introduces a potential model dependency. Validation using multi-model simulations, such as the Regional Aerosol Model Intercomparison Project (RAMIP) (Wilcox et al., 2023), is necessary for the next step when the data are available, to assess the Arctic responses to future changes in regional aerosols. Second, the choice of using CN, CN + SI, and CN + SI + SA perturbations was primary made to provide a stepwise assessment of the contributions from different regional emission changes. We acknowledge that this experimental setup implicitly assumes a certain degree of linearity in the climate system's response to regional aerosol perturbations, particularly when estimating the SI and SA components by differencing the responses from successive experiments. The nonlinearity in climate response could affect the quantitative magnitude of the estimated regional contributions from individual sources. Additionally, while the impact of regional aerosol changes on the Arctic temperature is discussed here, the feedback mechanisms involved have not been addressed in detail. Lastly, the varying magnitudes of Arctic temperature changes observed in our study primarily result from different magnitudes of regional aerosol perturbations. Comparing the impacts of similar magnitudes of aerosol perturbations across different regions could reveal the effects of emission locations on the Arctic climate, warranting further investigation.

Conflict of Interest

The authors declare no conflicts of interest relevant to this study.

Data Availability Statement

AOD data from the MODIS Deep Blue retrieval are available in Hsu et al. (2013a, 2013b). ERA5 reanalysis data can be obtained from Hersbach et al. (2020a, 2020b). CESM1 Large Ensemble Community Project (LENS) data is provided by Kay et al. (2015). The Community Earth System Model (CESM) source code is available in CESM Contributors (2013). The model results generated in this study can be accessed at Gao (2025).

Acknowledgments

This study was supported by National Key Research and Development Program of China (Grant 2024YFF0811400), the Natural Science Foundation of China (Grants 42521006 and 42475032), Jiangsu Innovation and Entrepreneurship Team (Grant JSSCTD202346), and Postgraduate Research Practice Innovation Program of Jiangsu Province (Grant KYCX25_1669). The Pacific Northwest National Laboratory (PNNL) is operated for the DOE by the Battelle Memorial Institute (contract no. DE-AC05-76RLO1830).

References

Alexeev, V. A., Langen, P. L., & Bates, J. R. (2005). Polar amplification of surface warming on an aquaplanet in "ghost forcing" experiments without sea ice feedbacks. *Climate Dynamics*, *24*(7–8), 655–666. https://doi.org/10.1007/s00382-005-0018-3

Beer, E., Eisenman, I., & Wagner, T. J. W. (2020). Polar amplification due to enhanced heat flux across the halocline. *Geophysical Research Letters*, *47*(4), e2019GL086706. https://doi.org/10.1029/2019GL086706

Bekryaev, R. V., Polyakov, I. V., & Alexeev, V. A. (2010). Role of polar amplification in long-term surface air temperature variations and modern arctic warming. *Journal of Climate*, *23*(14), 3888–3906. https://doi.org/10.1175/2010JCLI3297.1

Bintanja, R., Graversen, R. G., & Hazeleger, W. (2011). Arctic winter warming amplified by the thermal inversion and consequent low infrared cooling to space. *Nature Geoscience*, *4*(11), 758–761. https://doi.org/10.1038/ngeo1285

Bintanja, R., & Van Der Linden, E. C. (2013). The changing seasonal climate in the Arctic. *Scientific Reports*, *3*(1), 1556. https://doi.org/10.1038/srep01556

CESM Contributors. (2013). Community Earth System Model (CESM) source code (version 1) [Software]. *GitHub*. Retrieved from https://github.com/ESCOMP/CESM

Chen, X., & Dai, A. (2024). Quantifying contributions of external forcing and internal variability to arctic warming during 1900–2021. *Earth's Future*, *12*(5), e2023EF003734. https://doi.org/10.1029/2023EF003734

Chen, X., Kang, S., Hu, Y., & Yang, J. (2023). Temporal and spatial analysis of vegetation fire activity in the circum-Arctic during 2001–2020. *Research in Cold and Arid Regions*, *15*(1), 48–56. https://doi.org/10.1016/j.rcar.2023.03.002

Cheng, M.-T., Horng, C.-L., Su, Y.-R., Lin, L.-K., Lin, Y.-C., & Chou, C. C.-K. (2009). Particulate matter characteristics during agricultural waste burning in Taichung City, Taiwan. *Journal of Hazardous Materials*, *165*(1–3), 187–192. https://doi.org/10.1016/j.jhazmat.2008.09.101

Cherian, R., & Quaas, J. (2020). Trends in AOD, clouds, and cloud radiative effects in satellite data and CMIP5 and CMIP6 model simulations over aerosol source regions. *Geophysical Research Letters*, *47*(9), e2020GL087132. https://doi.org/10.1029/2020GL087132

Chin, M., Diehl, T., Tan, Q., Prospero, J. M., Kahn, R. A., Remer, L. A., et al. (2014). Multi-decadal aerosol variations from 1980 to 2009: A perspective from observations and a global model. *Atmospheric Chemistry and Physics*, *14*(7), 3657–3690. https://doi.org/10.5194/acp-14-3657-2014

Dagan, G., Stier, P., & Watson-Parris, D. (2021). An energetic view on the geographical dependence of the fast aerosol radiative effects on precipitation. *Journal of Geophysical Research: Atmospheres*, *126*(9), e2020JD033045. https://doi.org/10.1029/2020JD033045

Dai, A., Luo, D., Song, M., & Liu, J. (2019). Arctic amplification is caused by sea-ice loss under increasing CO_2. *Nature Communications*, *10*(1), 121. https://doi.org/10.1038/s41467-018-07954-9

Davy, R., & Outten, S. (2020). The Arctic surface climate in CMIP6: Status and developments since CMIP5. *Journal of Climate*, *33*(18), 8047–8068. https://doi.org/10.1175/JCLI-D-19-0990.1

England, M. R., Eisenman, I., Lutsko, N. J., & Wagner, T. J. W. (2021). The recent emergence of Arctic amplification. *Geophysical Research Letters*, *48*(15), e2021GL094086. https://doi.org/10.1029/2021GL094086

Friedlingstein, P., O'Sullivan, M., Jones, M. W., Andrew, R. M., Bakker, D. C. E., Hauck, J., et al. (2023). Global carbon budget 2023. *Earth System Science Data*, *15*(12), 5301–5369. https://doi.org/10.5194/essd-15-5301-2023

Gao, J. (2025). Data for "Increased aerosols from Siberian wildfires buffered Arctic warming during 2013–2019" [Dataset]. *Zenodo*. https://doi.org/10.5281/zenodo.15395337

Gao, J., Yang, Y., Wang, H., Wang, P., Li, B., Li, J., et al. (2023). Climate responses in China to domestic and foreign aerosol changes due to clean air actions during 2013–2019. *npj Climate and Atmospheric Science*, *6*(1), 160. https://doi.org/10.1038/s41612-023-00488-y

Gao, J., Yang, Y., Wang, H., Wang, P., Li, H., Li, M., et al. (2022). Fast climate responses to emission reductions in aerosol and ozone precursors in China during 2013–2017. *Atmospheric Chemistry and Physics*, *22*(11), 7131–7142. https://doi.org/10.5194/acp-22-7131-2022

Gettelman, A., Hannay, C., Bacmeister, J. T., Neale, R. B., Pendergrass, A. G., Danabasoglu, G., et al. (2019). High climate sensitivity in the community Earth System model version 2 (CESM2). *Geophysical Research Letters*, *46*(14), 8329–8337. https://doi.org/10.1029/2019GL083978

Gliß, J., Mortier, A., Schulz, M., Andrews, E., Balkanski, Y., Bauer, S. E., et al. (2021). AeroCom phase III multi-model evaluation of the aerosol life cycle and optical properties using ground- and space-based remote sensing as well as surface in situ observations. *Atmospheric Chemistry and Physics*, *21*(1), 87–128. https://doi.org/10.5194/acp-21-87-2021

Graversen, R. G., & Langen, P. L. (2019). On the role of the atmospheric energy transport in $2 \times CO_2$–Induced polar amplification in CESM1. *Journal of Climate*, *32*(13), 3941–3956. https://doi.org/10.1175/JCLI-D-18-0546.1

Guenther, A. B., Jiang, X., Heald, C. L., Sakulyanontvittaya, T., Duhl, T., Emmons, L. K., & Wang, X. (2012). The Model of Emissions of Gases and Aerosols from Nature version 2.1 (MEGAN2.1): An extended and updated framework for modeling biogenic emissions. *Geoscientific Model Development*, *5*(6), 1471–1492. https://doi.org/10.5194/gmd-5-1471-2012

Gui, K., Zhang, X., Che, H., Li, L., Zheng, Y., Zhao, H., et al. (2024). Future climate-driven escalation of Southeastern Siberia wildfires revealed by deep learning. *npj Climate and Atmospheric Science*, *7*(1), 263. https://doi.org/10.1038/s41612-024-00815-x

He, J., Zhang, Y., Glotfelty, T., He, R., Bennartz, R., Rausch, J., & Sartelet, K. (2015). Decadal simulation and comprehensive evaluation of CESM/CAM5.1 with advanced chemistry, aerosol microphysics, and aerosol-cloud interactions. *Journal of Advances in Modeling Earth Systems*, *7*(1), 110–141. https://doi.org/10.1002/2014MS000360

Hersbach, H., Bell, B., Berrisford, P., Hirahara, S., Horányi, A., Muñoz-Sabater, J., et al. (2020a). The ERA5 global reanalysis. *Quarterly Journal of the Royal Meteorological Society*, *146*(730), 1999–2049. https://doi.org/10.1002/qj.3803

Hersbach, H., Bell, B., Berrisford, P., Hirahara, S., Horányi, A., Muñoz-Sabater, J., et al. (2020b). ERA5 reanalysis [Dataset]. *Copernicus Climate Data Store. Pressure levels*: https://cds.climate.copernicus.eu/datasets/reanalysis-era5-pressure-levels-monthly-means

Hoesly, R. M., Smith, S. J., Feng, L., Klimont, Z., Janssens-Maenhout, G., Pitkanen, T., et al. (2018). Historical (1750–2014) anthropogenic emissions of reactive gases and aerosols from the Community Emissions Data System (CEDS). *Geoscientific Model Development*, *11*(1), 369–408. https://doi.org/10.5194/gmd-11-369-2018

Holland, M. M., & Bitz, C. M. (2003). Polar amplification of climate change in coupled models. *Climate Dynamics*, *21*(3), 221–232. https://doi.org/10.1007/s00382-003-0332-6

Hsu, N. C., Jeong, M.-J., Bettenhausen, C., Sayer, A. M., Hansell, R., Seftor, C. S., et al. (2013a). Enhanced Deep Blue aerosol retrieval algorithm: The second generation. *Journal of Geophysical Research: Atmospheres*, *118*(16), 9296–9315. https://doi.org/10.1002/jgrd.50712

Hsu, N. C., Jeong, M.-J., Bettenhausen, C., Sayer, A. M., Hansell, R. A., Seftor, C. S., et al. (2013b). MODIS Deep Blue aerosol products (version 6.1) [Dataset]. *NASA LAADS DAAC*. https://ladsweb.modaps.eosdis.nasa.gov/archive/allData/61/MOD08_M3/

Huang, J., Pan, X., Guo, X., & Li, G. (2018). Health impact of China's Air pollution prevention and control action plan: An analysis of national air quality monitoring and mortality data. *The Lancet Planetary Health*, *2*(7), e313–e323. https://doi.org/10.1016/S2542-5196(18)30141-4

Huang, X., Xue, L., Wang, Z., Liu, Y., Ding, K., & Ding, A. (2024). Escalating wildfires in siberia driven by climate feedbacks under a warming arctic in the 21st century. *AGU Advances*, *5*(4), e2023AV001151. https://doi.org/10.1029/2023AV001151

Hurrell, J. W., Holland, M. M., Gent, P. R., Ghan, S., Kay, J. E., Kushner, P. J., et al. (2013). The community Earth System model: A framework for collaborative research. *Bulletin of the American Meteorological Society*, *94*(9), 1339–1360. https://doi.org/10.1175/BAMS-D-12-00121.1

Hwang, Y.-T., Frierson, D. M. W., & Kay, J. E. (2011). Coupling between Arctic feedbacks and changes in poleward energy transport. *Geophysical Research Letters*, *38*(17), L17704. https://doi.org/10.1029/2011GL048546

IPCC. (2013). *Climate change 2013: The physical science basis. Contribution of working group I to the sixth assessment report of the intergovernmental panel on climate change*. Cambridge University Press.

IPCC. (2021). *Climate change 2021: The physical science basis. Contribution of working group I to the fifth assessment report of the intergovernmental panel on climate change*. Cambridge University Press.

Jenkins, M., & Dai, A. (2021). The impact of sea-ice loss on Arctic climate feedbacks and their role for Arctic amplification. *Geophysical Research Letters*, *48*(15), e2021GL094599. https://doi.org/10.1029/2021GL094599

Kay, J. E., Deser, C., Phillips, A., Mai, A., Hannay, C., Strand, G., et al. (2015). The CESM1 large ensemble project (LENS) [Dataset]. *NCAR Geoscience Data Exchange*. https://gdex.ucar.edu/datasets/d651027/

Larjavaara, M., Pennanen, J., & Tuomi, T. J. (2005). Lightning that ignites forest fires in Finland. *Agricultural and Forest Meteorology*, *132*(3–4), 171–180. https://doi.org/10.1016/j.agrformet.2005.07.005

Li, C., McLinden, C., Fioletov, V., Krotkov, N., Carn, S., Joiner, J., et al. (2017). India is overtaking China as the world's largest emitter of anthropogenic sulfur dioxide. *Scientific Reports*, *7*(1), 14304. https://doi.org/10.1038/s41598-017-14639-8

Liang, Y.-C., Polvani, L. M., & Mitevski, I. (2022). Arctic amplification, and its seasonal migration, over a wide range of abrupt CO2 forcing. *npj Climate and Atmospheric Science*, *5*(1), 14. https://doi.org/10.1038/s41612-022-00228-8

Liu, C., Yang, Y., Wang, H., Ren, L., Wei, J., Wang, P., & Liao, H. (2023). Influence of spatial dipole pattern in Asian aerosol changes on East Asian summer monsoon. *Journal of Climate*, *36*(6), 1575–1585. https://doi.org/10.1175/JCLI-D-22-0335.1

Liu, X., Ma, P.-L., Wang, H., Tilmes, S., Singh, B., Easter, R. C., et al. (2016). Description and evaluation of a new four-mode version of the Modal Aerosol Module (MAM4) within version 5.3 of the Community Atmosphere Model. *Geoscientific Model Development*, *9*(2), 505–522. https://doi.org/10.5194/gmd-9-505-2016

Liu, Y., Goodrick, S., & Heilman, W. (2014). Wildland fire emissions, carbon, and climate: Wildfire–climate interactions. *Forest Ecology and Management*, *317*, 80–96. https://doi.org/10.1016/j.foreco.2013.02.020

Luo, B., Luo, D., Dai, A., Xiao, C., Simmonds, I., Hanna, E., et al. (2024). Rapid summer Russian Arctic sea-ice loss enhances the risk of recent Eastern Siberian wildfires. *Nature Communications*, *15*(1), 5399. https://doi.org/10.1038/s41467-024-49677-0

Manoj, M. R., Satheesh, S. K., Moorthy, K. K., Gogoi, M. M., & Babu, S. S. (2019). Decreasing trend in Black carbon aerosols over the Indian Region. *Geophysical Research Letters*, *46*(5), 2903–2910. https://doi.org/10.1029/2018GL081666

McDuffie, E. E., Smith, S. J., O'Rourke, P., Tibrewal, K., Venkataraman, C., Marais, E. A., et al. (2020). A global anthropogenic emission inventory of atmospheric pollutants from sector- and fuel-specific sources (1970–2017): An application of the Community Emissions Data System (CEDS). *Earth System Science Data*, *12*(4), 3413–3442. https://doi.org/10.5194/essd-12-3413-2020

Miller, G. H., Alley, R. B., Brigham-Grette, J., Fitzpatrick, J. J., Polyak, L., Serreze, M. C., & White, J. W. C. (2010). Arctic amplification: Can the past constrain the future? *Quaternary Science Reviews*, *29*(15–16), 1779–1790. https://doi.org/10.1016/j.quascirev.2010.02.008

Pan, X., Ichoku, C., Chin, M., Bian, H., Darmenov, A., Colarco, P., et al. (2020). Six global biomass burning emission datasets: Intercomparison and application in one global aerosol model. *Atmospheric Chemistry and Physics*, *20*(2), 969–994. https://doi.org/10.5194/acp-20-969-2020

Persad, G., Samset, B. H., Wilcox, L. J., Allen, R. J., Bollasina, M. A., Booth, B. B. B., et al. (2023). Rapidly evolving aerosol emissions are a dangerous omission from near-term climate risk assessments. *Environmental Research: Climate*, *2*(3), 032001. https://doi.org/10.1088/2752-5295/acd6af

Persad, G. G., & Caldeira, K. (2018). Divergent global-scale temperature effects from identical aerosols emitted in different regions. *Nature Communications*, *9*(1), 3289. https://doi.org/10.1038/s41467-018-05838-6

Petäjä, T., Ganzei, K. S., Lappalainen, H. K., Tabakova, K., Makkonen, R., Räisänen, J., et al. (2021). Research agenda for the Russian Far East and utilization of multi-platform comprehensive environmental observations. *International Journal of Digital Earth*, *14*(3), 311–337. https://doi.org/10.1080/17538947.2020.1826589

Pithan, F., & Mauritsen, T. (2014). Arctic amplification dominated by temperature feedbacks in contemporary climate models. *Nature Geoscience*, *7*(3), 181–184. https://doi.org/10.1038/ngeo2071

Ponomarev, E. I., Zabrodin, A. N., Shvetsov, E. G., & Ponomareva, T. V. (2023). Wildfire intensity and fire emissions in Siberia. *Fire*, *6*(7), 246. https://doi.org/10.3390/fire6070246

Previdi, M., Smith, K. L., & Polvani, L. M. (2021). Arctic amplification of climate change: A review of underlying mechanisms. *Environmental Research Letters*, *16*(9), 093003. https://doi.org/10.1088/1748-9326/ac1c29

Rantanen, M., Karpechko, A. Y., Lipponen, A., Nordling, K., Hyvärinen, O., Ruosteenoja, K., et al. (2022). The Arctic has warmed nearly four times faster than the globe since 1979. *Communications Earth & Environment*, *3*(1), 168. https://doi.org/10.1038/s43247-022-00498-3

Ren, F., Lin, J., Xu, C., Adeniran, J. A., Wang, J., Martin, R. V., et al. (2024). Evaluation of CMIP6 model simulations of $PM_{2.5}$ and its components over China. *Geoscientific Model Development*, *17*(12), 4821–4836. https://doi.org/10.5194/gmd-17-4821-2024

Ren, L., Yang, Y., Wang, H., Wang, P., Yue, X., & Liao, H. (2022). Widespread wildfires over the Western United States in 2020 linked to emissions reductions during COVID-19. *Geophysical Research Letters*, *49*(15), e2022GL099308. https://doi.org/10.1029/2022GL099308

Ren, L., Yang, Y., Wang, H., Zhang, R., Wang, P., & Liao, H. (2020). Source attribution of Arctic black carbon and sulfate aerosols and associated Arctic surface warming during 1980–2018. *Atmospheric Chemistry and Physics*, *20*(14), 9067–9085. https://doi.org/10.5194/acp-20-9067-2020

Richardson, D., Black, A. S., Irving, D., Matear, R. J., Monselesan, D. P., Risbey, J. S., et al. (2022). Global increase in wildfire potential from compound fire weather and drought. *npj Climate and Atmospheric Science*, *5*(1), 23. https://doi.org/10.1038/s41612-022-00248-4

Samset, B. H., Lund, M. T., Bollasina, M., Myhre, G., & Wilcox, L. (2019). Emerging Asian aerosol patterns. *Nature Geoscience*, *12*(8), 582–584. https://doi.org/10.1038/s41561-019-0424-5

Sand, M., Berntsen, T. K., Von Salzen, K., Flanner, M. G., Langner, J., & Victor, D. G. (2016). Response of Arctic temperature to changes in emissions of short-lived climate forcers. *Nature Climate Change*, *6*(3), 286–289. https://doi.org/10.1038/nclimate2880

Screen, J. A., & Simmonds, I. (2010). The central role of diminishing sea ice in recent Arctic temperature amplification. *Nature*, *464*(7293), 1334–1337. https://doi.org/10.1038/nature09051

Semmler, T., Pithan, F., & Jung, T. (2020). Quantifying two-way influences between the Arctic and mid-latitudes through regionally increased CO2 concentrations in coupled climate simulations. *Climate Dynamics*, *54*(7–8), 3307–3321. https://doi.org/10.1007/s00382-020-05171-z

Serreze, M. C., Barrett, A. P., Stroeve, J. C., Kindig, D. N., & Holland, M. M. (2009). The emergence of surface-based Arctic amplification. *The Cryosphere*, *3*(1), 11–19. https://doi.org/10.5194/tc-3-11-2009

Serreze, M. C., & Francis, J. A. (2006). The Arctic amplification debate. *Climatic Change*, *76*(3–4), 241–264. https://doi.org/10.1007/s10584-005-9017-y

Smith, S. J., Van Aardenne, J., Klimont, Z., Andres, R. J., Volke, A., & Delgado Arias, S. (2011). Anthropogenic sulfur dioxide emissions: 1850–2005. *Atmospheric Chemistry and Physics*, *11*(3), 1101–1116. https://doi.org/10.5194/acp-11-1101-2011

Stjern, C. W., Lund, M. T., Samset, B. H., Myhre, G., Forster, P. M., Andrews, T., et al. (2019). Arctic amplification response to individual climate drivers. *Journal of Geophysical Research: Atmospheres*, *124*(13), 6698–6717. https://doi.org/10.1029/2018JD029726

Stuecker, M. F., Bitz, C. M., Armour, K. C., Proistosescu, C., Kang, S. M., Xie, S.-P., et al. (2018). Polar amplification dominated by local forcing and feedbacks. *Nature Climate Change*, *8*(12), 1076–1081. https://doi.org/10.1038/s41558-018-0339-y

Swart, N. C., Fyfe, J. C., Hawkins, E., Kay, J. E., & Jahn, A. (2015). Influence of internal variability on Arctic sea-ice trends. *Nature Climate Change*, *5*(2), 86–89. https://doi.org/10.1038/nclimate2483

Sweeney, A. J., Fu, Q., Po-Chedley, S., Wang, H., & Wang, M. (2023). Internal variability increased Arctic amplification during 1980–2022. *Geophysical Research Letters*, *50*(24), e2023GL106060. https://doi.org/10.1029/2023GL106060

Syphard, A. D., Radeloff, V. C., Keeley, J. E., Hawbaker, T. J., Clayton, M. K., Stewart, S. I., & Hammer, R. B. (2007). Human influence ON California fire regimes. *Ecological Applications*, *17*(5), 1388–1402. https://doi.org/10.1890/06-1128.1

Taylor, P. C., Cai, M., Hu, A., Meehl, J., Washington, W., & Zhang, G. J. (2013). A decomposition of feedback contributions to polar warming amplification. *Journal of Climate*, *26*(18), 7023–7043. https://doi.org/10.1175/JCLI-D-12-00696.1

Tomshin, O., & Solovyev, V. (2022). Spatio-temporal patterns of wildfires in Siberia during 2001–2020. *Geocarto International*, *37*(25), 7339–7357. https://doi.org/10.1080/10106049.2021.1973581

Tørseth, K., Aas, W., Breivik, K., Fjæraa, A. M., Fiebig, M., Hjellbrekke, A. G., et al. (2012). Introduction to the European Monitoring and Evaluation Programme (EMEP) and observed atmospheric composition change during 1972–2009. *Atmospheric Chemistry and Physics*, *12*(12), 5447–5481. https://doi.org/10.5194/acp-12-5447-2012

Tsigaridis, K., Daskalakis, N., Kanakidou, M., Adams, P. J., Artaxo, P., Bahadur, R., et al. (2014). The AeroCom evaluation and intercomparison of organic aerosol in global models. *Atmospheric Chemistry and Physics*, *14*(19), 10845–10895. https://doi.org/10.5194/acp-14-10845-2014

Turnock, S. T., Allen, R. J., Andrews, M., Bauer, S. E., Deushi, M., Emmons, L., et al. (2020). Historical and future changes in air pollutants from CMIP6 models. *Atmospheric Chemistry and Physics*, *20*(23), 14547–14579. https://doi.org/10.5194/acp-20-14547-2020

Van Der Werf, G. R., Randerson, J. T., Giglio, L., Van Leeuwen, T. T., Chen, Y., Rogers, B. M., et al. (2017). Global fire emissions estimates during 1997–2016. *Earth System Science Data*, *9*(2), 697–720. https://doi.org/10.5194/essd-9-697-2017

Wang, P., Yang, Y., Xue, D., Ren, L., Tang, J., Leung, L. R., & Liao, H. (2023). Aerosols overtake greenhouse gases causing a warmer climate and more weather extremes toward carbon neutrality. *Nature Communications*, *14*(1), 7257. https://doi.org/10.1038/s41467-023-42891-2

Wang, Q., Fan, X., & Wang, M. (2016). Evidence of high-elevation amplification versus Arctic amplification. *Scientific Reports*, *6*(1), 19219. https://doi.org/10.1038/srep19219

Wilcox, L. J., Allen, R. J., Samset, B. H., Bollasina, M. A., Griffiths, P. T., Keeble, J., et al. (2023). The Regional Aerosol Model Intercomparison Project (RAMIP). *Geoscientific Model Development*, *16*(15), 4451–4479. https://doi.org/10.5194/gmd-16-4451-2023

Williams, A. I. L., Watson-Parris, D., Dagan, G., & Stier, P. (2023). Dependence of fast changes in global and local precipitation on the geographical location of absorbing aerosol. *Journal of Climate*, *36*(18), 6163–6176. https://doi.org/10.1175/JCLI-D-23-0022.1

Woods, C., & Caballero, R. (2016). The role of moist intrusions in Winter arctic warming and Sea ice decline. *Journal of Climate*, *29*(12), 4473–4485. https://doi.org/10.1175/JCLI-D-15-0773.1

Wu, Y.-T., Liang, Y.-C., Previdi, M., Polvani, L. M., England, M. R., Sigmond, M., & Lo, M.-H. (2024). Stronger Arctic amplification from anthropogenic aerosols than from greenhouse gases. *npj Climate and Atmospheric Science*, *7*(1), 142. https://doi.org/10.1038/s41612-024-00696-0

Xing, J., & Wang, M. (2023). Trend and drivers of satellite-detected burned area changes across Arctic region since the 21st century. *Journal of Geophysical Research: Atmospheres*, *128*(19), e2023JD038946. https://doi.org/10.1029/2023JD038946

Yang, Y., Wang, H., Smith, S. J., Easter, R. C., & Rasch, P. J. (2018). Sulfate aerosol in the Arctic: Source attribution and radiative forcing. *Journal of Geophysical Research: Atmospheres*, *123*(3), 1899–1918. https://doi.org/10.1002/2017JD027298

Zacharakis, I., & Tsihrintzis, V. A. (2023). Integrated wildfire danger models and factors: A review. *Science of the Total Environment*, *899*, 165704. https://doi.org/10.1016/j.scitotenv.2023.165704

Zhang, R., Wang, H., Fu, Q., Pendergrass, A. G., Wang, M., Yang, Y., et al. (2018). Local radiative feedbacks over the arctic based on observed short-term climate variations. *Geophysical Research Letters*, *45*(11), 5761–5770. https://doi.org/10.1029/2018GL077852

Zhang, R., Wang, H., Fu, Q., & Rasch, P. J. (2020). Assessing global and local radiative feedbacks based on AGCM simulations for 1980–2014/2017. *Geophysical Research Letters*, *47*(12), e2020GL088063. https://doi.org/10.1029/2020GL088063

Zhang, R., Wang, H., Fu, Q., Rasch, P. J., Wu, M., & Maslowski, W. (2021). Understanding the cold season arctic surface warming trend in recent decades. *Geophysical Research Letters*, *48*(19), e2021GL094878. https://doi.org/10.1029/2021GL094878

Zheng, B., Ciais, P., Chevallier, F., Yang, H., Canadell, J. G., Chen, Y., et al. (2023). Record-high CO_2 emissions from boreal fires in 2021. *Science*, *379*(6635), 912–917. https://doi.org/10.1126/science.ade0805

Zheng, B., Tong, D., Li, M., Liu, F., Hong, C., Geng, G., et al. (2018). Trends in China's anthropogenic emissions since 2010 as the consequence of clean air actions. *Atmospheric Chemistry and Physics*, *18*(19), 14095–14111. https://doi.org/10.5194/acp-18-14095-2018

Zhong, Q., Schutgens, N., Veraverbeke, S., & Van Der Werf, G. R. (2024). Increasing aerosol emissions from boreal biomass burning exacerbate Arctic warming. *Nature Climate Change*, *14*(12), 1275–1281. https://doi.org/10.1038/s41558-024-02176-y

Zhou, S.-N., Liang, Y.-C., Mitevski, I., & Polvani, L. M. (2023). Stronger Arctic amplification produced by decreasing, not increasing, CO_2 concentrations. *Environmental Research: Climate*, *2*(4), 045001. https://doi.org/10.1088/2752-5295/aceea2